Human-computer Interaction for Hybrid Carving

Amit Zoran
Responsive Environments
MIT Media Lab
amitz@media.mit.edu

Roy Shilkrot
Fluid Interfaces
MIT Media Lab
roys@media.mit.edu

Joseph Paradiso
Responsive Environments
MIT Media Lab
joep@media.mit.edu

ABSTRACT
In this paper we explore human-computer interaction for carving, building upon our previous work with the FreeD digital sculpting device. We contribute a new tool design (FreeD V2), with a novel set of interaction techniques for the fabrication of static models: personalized toolpaths, manual overriding, and physical merging of virtual models. We also present techniques for fabricating dynamic models, which may be altered directly or parametrically during fabrication. We demonstrate a semi-autonomous operation and evaluate the performance of the tool. We end by discussing synergistic cooperation between human and machine to ensure accuracy while preserving the expressiveness of manual practice.

Author Keywords
Computer-Aided Design (CAD); Craft; Digital Fabrication; Carving; Milling.

ACM Classification Keywords
H.5.2 Information interfaces and presentation: User Interfaces; I.3.8 Computer Graphics: Applications

INTRODUCTION
This paper contributes an application of a digital sculpting device for hybrid carving, using a revised version of the FreeD tool (FreeD V2), previously discussed in [21]. FreeD enabled users to make physical artifacts with virtual control, and FreeD V2 adds manual and computational design modification *during* fabrication, rendering a unique 3D model directly in a physical material. Our intention is to explore a territory where artifacts are produced in a collaborative effort between human and machine, incorporating subjective decision-making in the fabrication process and blurring the line between design and fabrication.

In the course of our work, we discuss different hybrid interaction methodologies. Not only does the tool assist inexperienced makers carving complex 3D objects (static-model mode, see Figure 1), it also enables personalizing and changing of the underlying model (dynamic model mode). In the latter case, FreeD doubles as an input device, where the user moves and the computer reacts. We present several novel modes of interaction such as switching between virtual models through the work; overriding the computer; deforming a virtual model while making it; or searching interactively for an optimal parametric model. In addition, the new tool can operate independently for tasks such as semi-automatic texture rendering.

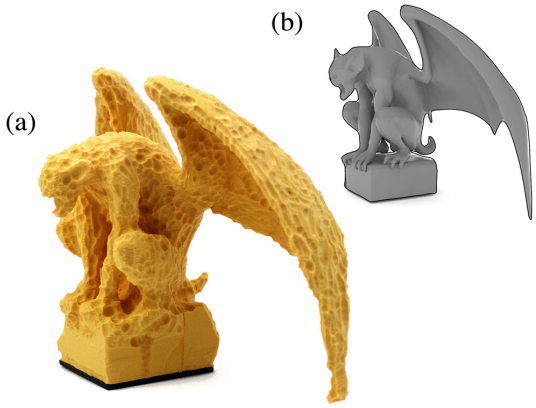

Figure 1. A gargoyle sculpture (with a wingspan of 280mm) made with the FreeD V2 (a) based on a complex CAD model (b).

In the next section, we discuss our previous efforts and related work, and in the subsequent section titled *The FreeD V2 Design*, we present the new version of the FreeD, focusing on revisions from the early version. In *Modes of collaboration and interaction*, we present three operational modes: static (rigid) model, dynamic model (a computational virtual model that responds to the users actions), and a semi-autonomous mode of tool operation. Finally, in *Performance and exploration*, we discuss the experience of working with the tool.

RELATED WORK
Today, we tend to see design and fabrication as two distinct digital practices, where design is the creative stage and fabrication is the automatic production stage. Unlike in contemporary digital practice, in traditional craft, the intuitive engagement in fabrication directly influences the result [11]. Following traditional craft practices and carving techniques, we presented the FreeD, a handheld digital milling device, monitored by a computer that controls the speed and alignment of the shaft while preserving the maker's gestural freedom. In [21] we discussed our concept, compared traditional craft and modern processes, and reviewed related work in artistic expression and handheld digital fabrication tools.

Relevant concepts in hybrid design and fabrication were previously implemented by digitally monitored 3D clay sculpt-

UIST'13, October 08 - 11, 2013, St. Andrews, United Kingdom.

http://dx.doi.org/10.1145/2501988.2502023

ing with bare hands or manual tools [16, 14]. We found CopyCAD by Follmer et al. [7] especially interesting, as it allows users to copy 2D elements of physical objects, then reassemble and re-fabricate these elements in a new 2D shape.

FreeD V2 can be used to modify the virtual model during fabrication. Gustafson et al. studied the use of hand-gestures in free-air as a control input for a virtual shape without visual feedback [8], Song et al. [18] used annotation squiggles with a pen, Arisandi et al. [3] employed specialized handheld tools, and Cho et al. [5] used a depth camera to track hand-gestures in shaping a virtual object using a virtual pottery wheel. Recently, similar ideas were integrated with fabrication technologies, such as laser cutters [10, 12], a RepRap 3D printer [13] and specialized fabricators [20].

THE FREED V2 DESIGN

In this section, we introduce the new design to readers unfamiliar with our previous work and detail its additional capabilities: an overriding button, LEDs, sonic control, and an addition of two degrees of freedom (DOF) of shaft deflection, which allows additional semi-automatic movements. The device is one element of a system (see Figure 2) that contains the handheld tool, a magnetic motion tracking system (MMTS), the fabricated object, a computer, and software distributed over the laptop and the tool. The tool is usually held with a single hand, while the user is free to move it in 3D, limited only by the length of power cables and the MMTS.

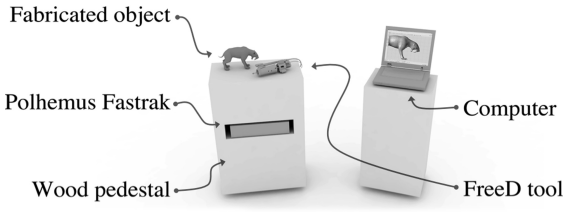

Figure 2. The FreeD, work environment, computer, and MMTS.

Tool design and motor control

The FreeD V2 contains a custom milling mechanism (spindle) built on top of a long shaft (Figure 4) with a 12V DC motor (Micro-Drives M2232U12VCS with up to 10,000 RPM with no load, and up to 5.2mNm torque). A custom 3D bearing mechanism is located underneath the handle, sitting above the titanium shaft and enabling three DOF movements at an approximate spherical volume of 20 mm (see Figure 3). Three servomotors (MKS 6125 mini servos, with up to 5.8 kg-cm for 6V), aligned perpendicular to the shaft near the spindle motor, determine the shaft's position. An electronic circuit on the PCB (with an ATmega328 microprocessor and a MC33926 motor driver, powered with 5V and 12V signals) communicates with the computer via Bluetooth to control the shaft movement and the spindle speed.

A force-sensing resistor (FSR) sensor is located on the handle, allowing the user to override the computer. The DC motor speed (Sp, where 1 is the maximum value) is a function of the pressure read from the FSR (Pr, where 1 is maximum value) and the risk to the model (Rs, 1 is maximal risk - see

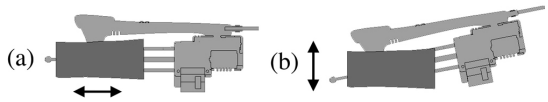

Figure 3. The multiple-axis bearing allows the milling bit to move in 3 degrees of freedom: 2 in the carving-plane, and a forward-backward motion.

Figure 5 (a)-(c)):

$$Sp = 1 - Rs(1 - Pr) \quad (1)$$

Two LEDs are located on the tool to provide the user with visual feedback. The first LED's blinking frequency correlates to the pressure detected by the FSR. The second LED corresponds to the distance between the bit and the surface of the model (when the bit touches the model's surface, the light is constant). In addition, the operating frequency of the DC motor (PWM), controlled by the motor-driver, changes from ultrasonic to an audible range (arround 2KHz) to give the user an alarm when the bit is within 4mm of the model surface.

The major part of the computation is done on a computer (Alienware M14x Laptop with i7-3740QM Intel core, 12GB DDR3, and 2GB NVIDIA GeForce GT 650M graphic card). The computer also provides the user with a visual feedback on the screen (see Figure 5 (d-f)). For tracking (MMTS) we use the Polhemus FASTRAK system, an AC 6D system that has low latency (4ms), high static accuracy (position 0.76mm / orientation 0.15° RMS), and high refresh rate (120Hz).

On the computer, where the virtual model resides, the software runs in Grasshopper and Rhino. The input is the 6D location and orientation of the tool, and the outputs are commands to the control PCB on the FreeD. A prediction of the next position of the bit is extrapolated by a spline of the 4th order (using the current location and the 3 previous ones). The software calculates the distances (D) to the CAD model (using rhinoscript MeshCP()) from both the current location and the predicted one, estimating which point puts the model at higher risk (i.e., which is closer to the model). While the DC motor's speed is calculated on the tool as a factor of Pr and Rs, the latter is calculated by the main control software (values in mm):

$$Rs = \begin{cases} 0 & \text{if } D <= 100 \ \ and \ \ D > 4; \\ D/8 & \text{if } D <= 4 \ \ and \ \ D > 0; \\ 1 & \text{elsewhere.} \end{cases} \quad (2)$$

The default shaft position is fully extended, with a 20mm potential to absorb the offset and retract. Unlike our early work, in the FreeD V2 we now use the servos for independent tool operation rather than as a penetration protection mechanism.

Method of Operation

Operation of the FreeD V2 is similar to that discussed earlier: the user sits in front of the material (Balsa foam), which is attached to a wooden stand (see Figure 2). The physical working area is calibrated to the virtual workspace. She is free to investigate any milling approach, such as milling lines, drilling holes, trimming surfaces, or using an arbitrary

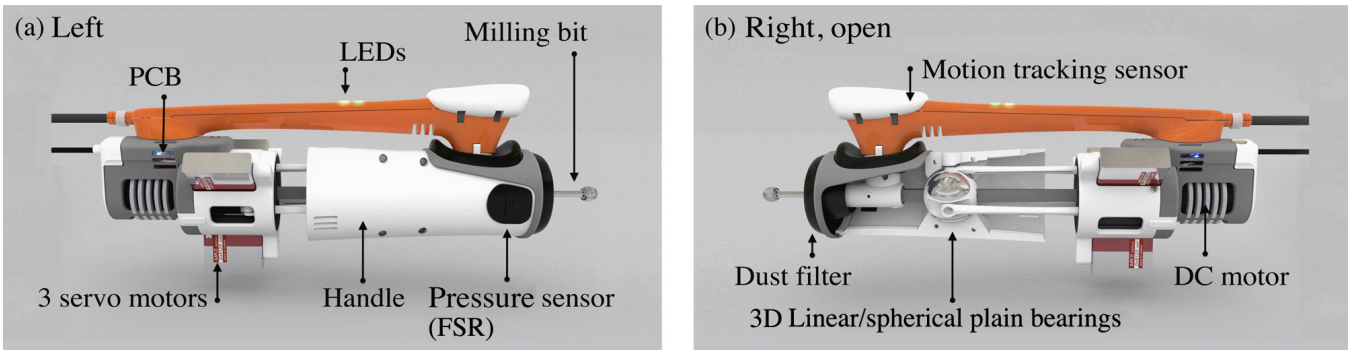

Figure 4. FreeD V2 is a handheld digital milling tool: (a) a left view of the tool, with its main components, and (b) a right view of the opened device.

pattern. The computer slows down the spindle as the bit approaches the model, stopping it completely before it penetrates the virtual model (see Figure 5 (d-f)). This enables the user to cut along the boundary of the virtual model where desired. She can leave parts of the model unfinished or override the computer using the pressure sensor. Further, in some modes of operation, the system can dynamically alter the model based on user actions or operate autonomously.

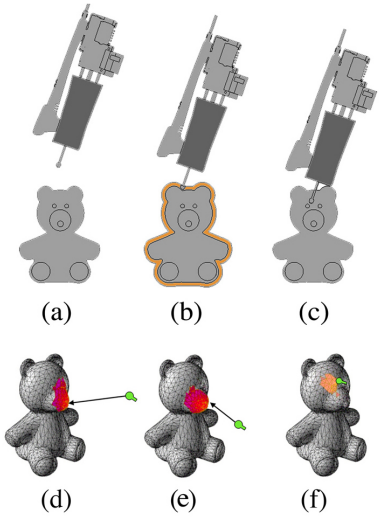

Figure 5. Risk management with the FreeD. (a-c) Low, High and penetration level of risk. (d-f) Heatmap visualization of the risk zone.

MODES OF COLLABORATION AND INTERACTION

In this section, we survey several original interaction modes with FreeD V2: the static CAD model mode where the computer assists only by preventing the user from damaging the model (the first part of this section, *Toolpath personalization*, was partially discussed in our early work); a dynamic mode where the computer numerically controls the model, responding to the user's actions; and the autonomous mode where the computer can operate independently of the user for tasks such as semi-automatic texture rendering. Together, these modes span a new space, where both human and computer work in synergy and contribute to the final product.

Fabrication of static models

In the fabrication of a static model, the user cannot alter the CAD model, and the boundary of the virtual object remains static. This approach resembles traditional digital fabrication technologies, where the virtual model is fixed and prepared beforehand. Here however, the user (rather than an automatic process) determines the toolpath. This enables personalization of the work, and may also circumvent complicated CAD challenges such as merging 3D elements into a single object.

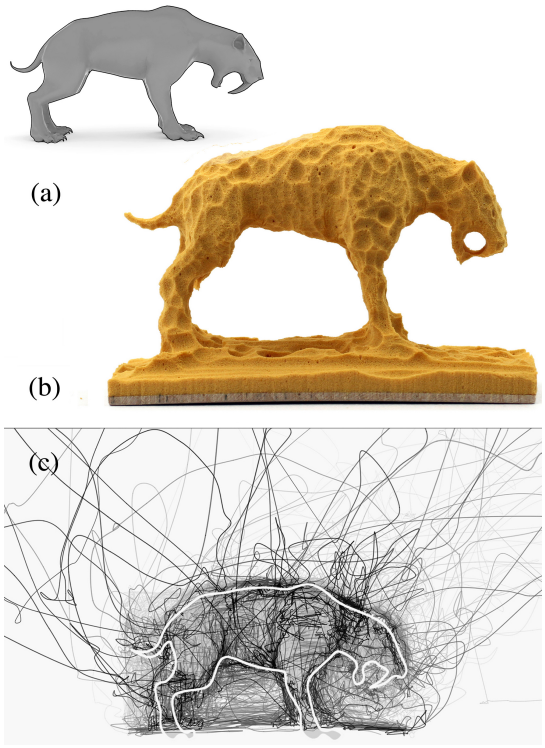

Figure 6. Sculpting a static model of a sabertooth tiger (80 min fabrication time, length 125mm). (a) The 3D model, (b) the end result of the sculping process, (c) and the toolpath projection. The tool is capable of achieving a smoother surface (see Figure 16), with deliberate intent.

Toolpath personalization

As discussed earlier, FreeD gives the user direct control over the milling toolpath. The final surface smoothness and resolution are determined by the size and shape of the endmill and

the toolpath. Usually in fabrication, a manual process renders a chaotic surface pattern whereas an automatic process renders an organized network of marks. This is mainly because in a manual toolpath, a product of the maker's dexterity and patience, the operation never repeats itself and evolves into a unique texture, for example in the fabrication of a saber-tooth tiger model (Figure 6 (a)). The final texture (b) reflects the user toolpath (c), properties of the material, milling bit size, and latency of the system. The parts left unfinished (the legs) demonstrate decisions made during the work.

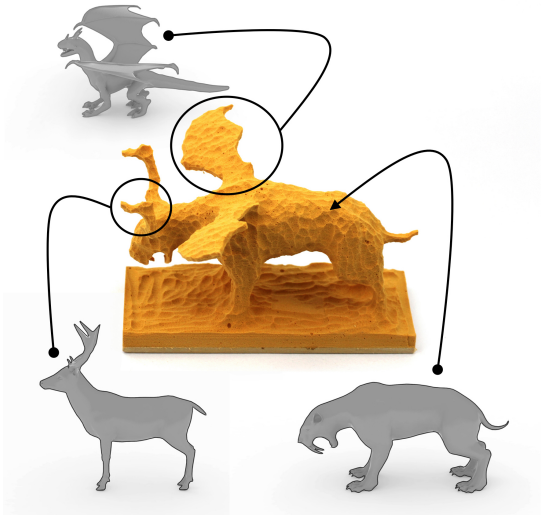

Figure 7. Hybridization of meshes while sculpting (100 min fabrication time, model length 120mm). The final 3D shape does not exist virtually; it only exists in the fabricated model.

Physical merging

As FreeD encourages the user to work creatively and intuitively, the user can manually switch between different reference virtual models *during* the work. The fusion of these models need not be determined numerically but physically, relinquishing the need to solve mesh intersection problems in making a single CAD model, as in the merging of a saber-tooth tiger with dragon wings and deer horns (Figure 7).

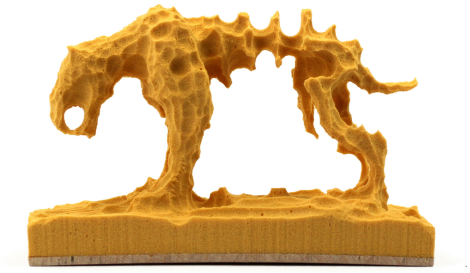

Figure 8. The result of overriding computer guidance is a completely different design (90 min fabrication time, model length 120mm). The artist takes risks and produces a unique artifact.

Manual override

Here, we present an approach foreign to most digital fabrication methods: allowing *intentional destruction* of the fabricated model. By overwriting the computer, the user minimizes digital control on the shaft while keeping the advantage of digital guidance with an aural alarm and LED. In addition to leaving parts unfinished, the maker can intentionally "damage" the model, working around or *inside* the virtual shape, allowing for physical improvisation. Beyond Figure 6b, in Figure 8, the user continued to manually remove parts of the model to achieve a unique artifact.

Fabrication of dynamic models

Today, digital fabrication technologies require models to be designed beforehand and no changes can be made during fabrication, as in the static approach presented in the last section. In contrast, craftpersons are free to deform the subject during the creation process, as long as the remaining material allows. Aiming to recreate this freedom, we present a novel capability to allow the modification of dynamic virtual models during fabrication, exploring three types of interaction with dynamic models: Direct shape deformation, Volume occupancy optimization, and Data-driven shape exploration.

Direct shape deformation

The first order dynamics in our interaction model is to allow for direct deformation of a CAD model. Unlike manual overriding of a static model, in direct shape deformation the computer keeps track of subtracted material: when the user presses the override button and penetrates the virtual model, the computer deforms the mesh to ameliorate the penetration.

Recent related methods of mesh deformation [19] seek to preserve local features under deformation. Here, we used a simplified weighting scheme for local deformation with respect to the user's action. As the weights for the offset vector of vertices ($\vec{O_v}$, where v is the vertex index) we use a Gaussian decay over the distance from the nearest vertex to the bit, to create an effect of a smooth deformation:

$$\vec{O_v} = \vec{T_v} * e^{\frac{-(d_v/S)^2}{0.005(10-Pr)^2}} \quad (3)$$

Where Pr is the value read from the override FSR button (0 is no pressure and 1 is maximal pressure), $\vec{T}$ is the penetration vector (the vector between the point of first contact to the deepest bit position), d_v is the distance from v to the penetration point, and S is the number of affected vertices, a constant number that can be defined by the user (and thus define the affected area). See Figure 9 for an example of deforming a mesh while fabricating.

Volume occupancy optimization

Further examining the art of carving, we face a common challenge: fitting a shape to a given volume of material, for example in the case of an irregular piece of wood, where the artist may try to maximize the volume of the shape while bounded by the material. FreeD allows the user to work in this fashion, using optimization of volume occupancy.

We illustrate the idea of volume occupancy optimization through a simple parametric bowl with three parameters: inner and outer radii (r_i, r_o) and height (c). Let us denote $\Theta = \{r_o, r_{in}, c\}$. Spheres and cubes were used to create the model of the bowl with constructive solid geometry (CSG) boolean operations (using the Carve CSG library [17]). See Figure 10 (e) for examples of parametic bowls.

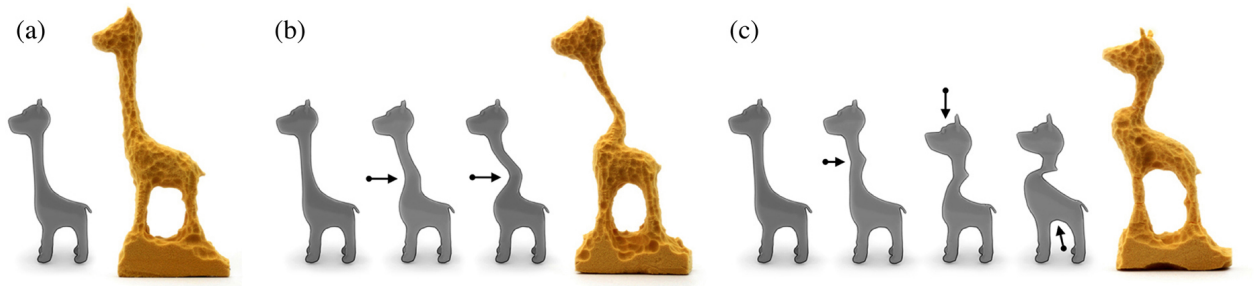

Figure 9. Model deformation while carving using the override mechanism. The model is smoothly deformed in proportion to the bit's penetration of the material. (a) The original model, (b) deformation from the left, (c) and deformations of the model from multiple directions.

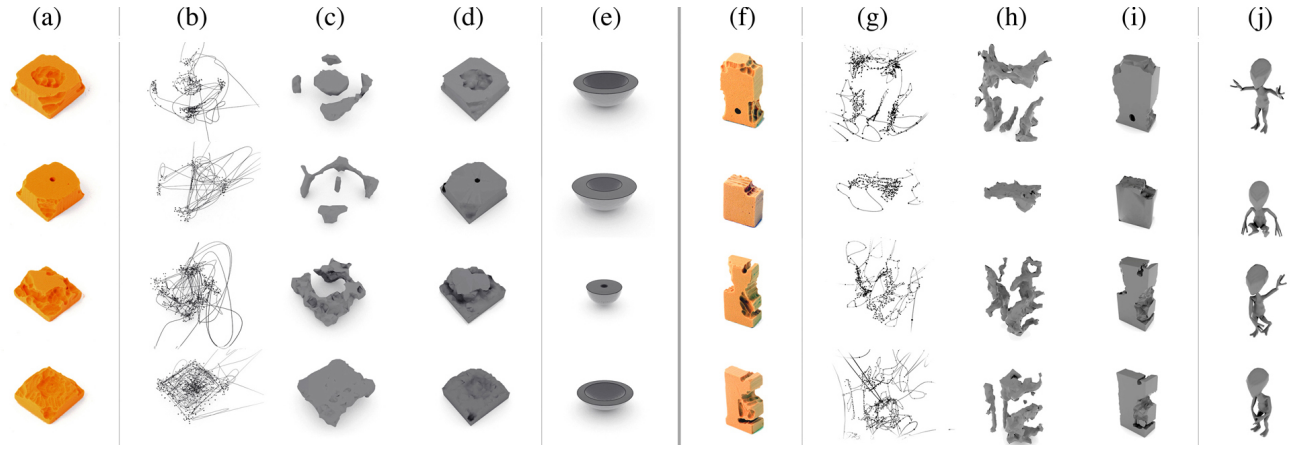

Figure 10. An initial iteration in a parametric fitting process of bowl and humanoid forms: (a), (f) the physical carved material, (b), (g) renderings of the toolpath, (c), (h) simulations of the material *removed* by the tool, (d), (i) simulations of the remaining material, (e), (j) result of the fitting algorithm.

In order to fit a shape in the material, we first determine the remaining volume. After the FreeD carves out a part of the material, the toolpath is bounded so only the points inside the volume in question are left (see Figure 10 (b)). Each point describes only the center of the bit, therefore 10 points were randomly sampled on a sphere with radius 3.2mm (the real bit size) to simulate the whole bit as it passed through space. A solid shape is created out of the point cloud using the Alpha Shapes method [6] (see Figure 10-(c)). Once the removed portion is established, the remaining volume is easily obtained with a boolean CSG operation (see Figure 10-(d)).

A parametric bowl is then fitted inside the remaining volume by a score function vector, whose norm should be minimized:

$$f_1(\Theta) = w_1 * V_{remain}(\Theta)$$
$$f_2(\Theta) = w_2 * V_{out}(\Theta)$$
$$f_3(\Theta) = w_3 * (1 - c)$$
$$f_4(\Theta) = w_4 * (1 - r_{in})$$
$$F(\Theta) = [f_1(\Theta); f_2(\Theta); f_3(\Theta); f_4(\Theta)]$$

The $V_{remain}(\Theta)$ marks the remaining volume of material after the bowl was subtracted and $V_{out}(\Theta)$ marks the volume that the bowl takes *outside* the remaining volume, i.e. out in the air. These measures should be minimized so to maximize occupancy and minimize escape. The bowl is made as high and thick as possible using the final two residuals. We used a non-linear least-squares solver [2] to find the solution for the canonical optimization problem: $\arg\min_{\Theta} \|F(\Theta)\|^2$. Due to the CSG operations, the function is evaluated numerically.

Data-driven shape exploration

In this dynamic-model mode we strive to simulate the unbounded amount of possible outcomes that manual carving allows. Using a vast database, the tool guides users while exploring the shape-space in an interactive process.

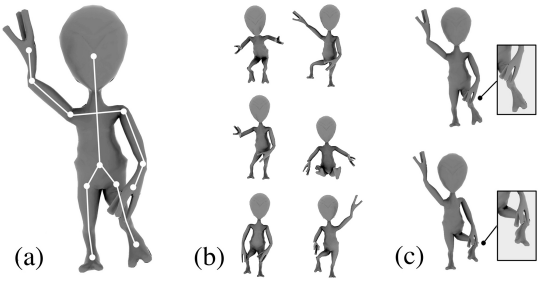

Figure 11. The parametric skeleton model of a humanoid creature: (a) skeleton of 14 joints, (b) sample of the database of possible poses, (c) fine-tuning process recovers the best pose to fit the remaining material.

We work with a hierarchical database of over 4000 examples of human poses that were recorded with the Kinect sensor via the OpenNI software stack [1]. The poses were clustered using a K-Means variant, to 50 clusters (meta-poses) of varying sizes, using WEKA [9]. Then, we use the method from [4]

to auto-rig the humanoid alien model to a skeleton model that corresponds with the Kinect. For deformation of the mesh, we used the canonical Linear Blend Skinning method. Figure 11-(a) and (b) illustrates the database of skeleton poses.

The process of finding the remaining volume (see the previous section) is repeated. Then, an exhaustive search over the database is performed to find the meta-pose that has the least amount of escape from the remaining volume (V_{out}), followed by a search within the best-found cluster. Several options for advancement are presented to the user to choose from in each iteration. After the database search, fine tuning ensues, for the position of the limbs and for small translations of the entire shape in respect to the volume. Figure 11-(c) shows an example of finely tuning the alien pose.

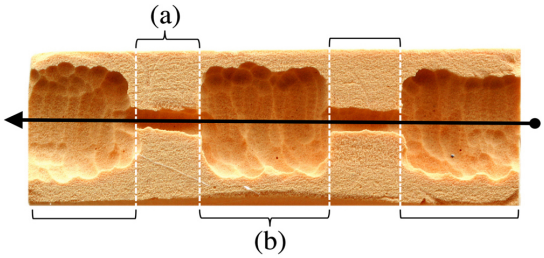

Figure 12. Automatic tool operation in a straight line. In (a) regions there is no autonomous movement, while in (b) regions the shaft programmatically removes more material resulting in a bigger *virtual bit*.

Autonomous operation mode

Digital fabrication technologies incorporate several degrees of automatic motion, while common hand-held devices do not automatically move but are manually controlled. The use of automatic motion in hand-held devices is rarely considered. Lately this is changing, as was demonstrated by Rivers et al. [15], by integrating 2D actuation mechanism to correct the user's path, and in [21] , where shaft retraction prevents the user from accidental penetration of the model.

An independent actuation of the shaft operates semi-autonomously: while the user holds FreeD and makes large-scale movements, the tool makes autonomous smaller-scale movements. For example, the tool is operated as a semi-autonomous milling device (CNC, see Figure 12). In Figure 13 we demonstrate a semi-autonomous texture rendering: when the bit is closer than 4mm to the fur segment, the servos operate with a linear pecking movement (4Hz, 5mm movement range) to achieve a fur texture. The user continues to operate the tool freely, unconstrained by the shaft actuation.

PERFORMANCE AND EXPLORATION

In this section, we first present statistical performance measurements collected while working with the FreeD V2, before discussing our experience using the tool.

System performance

The FreeD V2 system was used (mostly by us) in the fabrication of 11 complete artifacts, in addition to several 3D sketches and a few preliminary sculptures in our early studies. We tested the tool with carving in both high and low

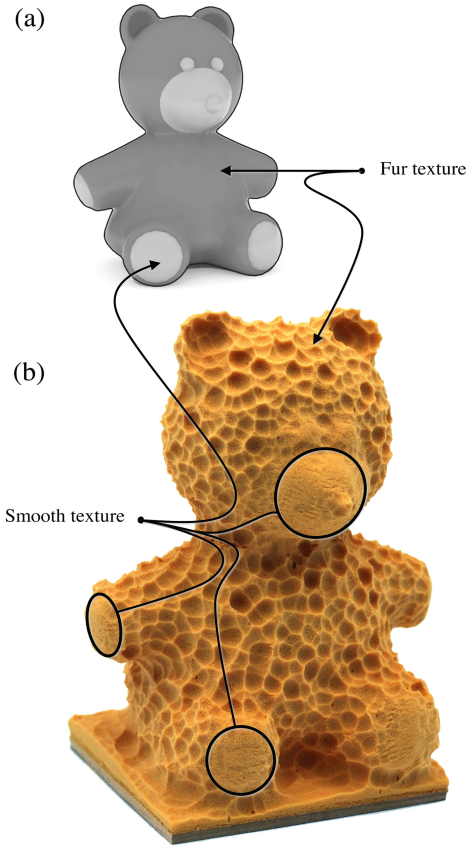

Figure 13. Teddy bear model (height 147mm) (a) embellished with fur textures. The mesh is encoded with a rough or smooth texture. The rough texture causes the shaft to move back and forth, creating dimples in the material that simulate fur (b).

density balsa foams, basswood, and carving wax. All of the studies presented in this paper were done in foam, since it took up to 10 times longer to machine wax and wood. The control software updated at a frame rate varying between 10 to 20 frames per second (FPS). We worked with mesh models of 150 vertices (humanoid) to 5370 vertices (gargoyle), lengths between 120mm (giraffe) to 280mm (gargoyle), and with production times of 40 minutes (giraffe) to 5 hours (gargoyle). The static-bit accuracy (measured by holding the bit in one place while rotating the tool around it) varies between 0.05 mm RMS (20cm from the magnetic field generator) to 0.4mm RMS (70cm away).

While in our work we seek personalization of artifact rather than production accuracy, here we test how accurately the FreeD can reconstruct a predesigned virtual model. The surface accuracy depends on the frame rate, tool movement speed, and material density. For example, with 15 FPS and 350mm/sec attack speed, the bit penetrated 3.5mm in a dense balsa foam before the system shut down the spindle rotation.

To empirically evaluate the accuracy of FreeD V2 we designed a model with non-straight angles and a sphere (Figure 14 (a)), fabricated it with FreeD, and then scanned it with Konica Minolta VIVID 910 scanner so to computationally es-

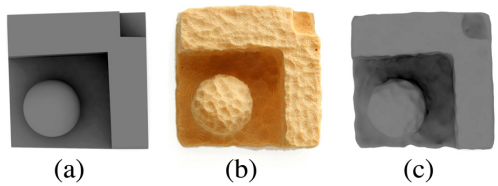

Figure 14. An examination of the FreeD V2's accuracy measure. (a) the virtual model (53mm length) , (b) the model fabricated with FreeD, (c) a 3D scanning of the fabrication. The RMS error is less than 0.5mm.

timate the error. We present the following results only to give a general sense of accuracy, as the adherence of the resulting surface to the virtual model is greatly a factor of the maker's dexterity and patience, a complex concept to quantify. The resulting error was smaller than 0.5mm RMS (samples for this measurement were taken within a grid of less than 1mm resolution). As expected because of the bit size, FreeD fails to clear out material from sharp corners; however all subtractive fabrication methods suffer from this drawback.

Experimentation

Here we discuss the making of a larger-scale model that incorporates most of the functionalities of the tool. We made a humanoid model, an alien figure, which features a large head and elongated arms. The work began by interactively exploring the skeleton database in the same manner we discussed earlier (see section). Figure 15 (b-d) shows the different poses fetched from the database while carving out material. When a satisfying pose was found, we began removing larger chunks of material. Using the shape deformation method described earlier, we created a dent in the model to emphasize the sideways motion of the hips (see Figure 15-(e)). We then kept removing material until the general form was fleshed out (see Figure 15-(f) for an illustration) and moved on to texturing and decorating. On the computer we set the alien's head to have a rough texture that will resemble hair. Finally, we used the override mechanism to create completely unguided carvings of the mouth and navel, and decided to leave part of the model unfinished.

Discussion

Extended user studies will be conducted to validate the tool's capabilities in supporting creative processes. Yet, using the tool ourselves and allowing five other participants to collaborate on single carving (see Figure 16), we have a few initial reflections. In projects presented in this paper, the tool was guided along lines away from the object, removing material from one side to another. When the model becomes recognizable, the operation changed to tracking the surface manifolds. Changes in spindle speed, when the bit approaches the model surface, inform the users on the relative location of the tool with respect to the model and help build intuition. Several participants noted it took them a while to trust the tool in protecting the object from a wrong movement.

On the screen, a virtual mark represents the current position of the FreeDs milling bit (see Figure 5 (d)-(f)). Occasionally, we relied on this mark in the initial stage where the virtual shape is not yet revealed in the raw material. However, the

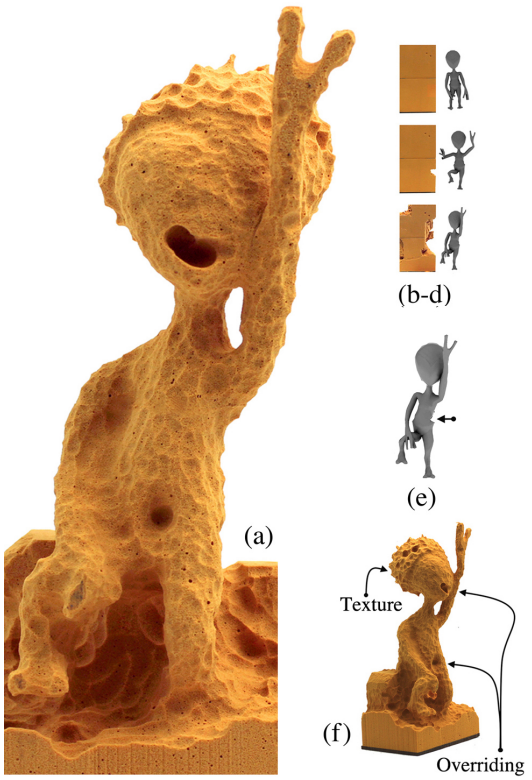

Figure 15. Fabrication of a humanoid model (height 222mm) illustrating all methods. (a) The final artifact. (b-d) Evolution of the model as material is removed. (e) Smooth deformation. (f) Texturing hair and deliberate penetration of the model to carve a mouth and navel.

main limitation of the FreeD, as indicated by several users, is a lack in visual feedback of the virtual model projected on the material. On the other hand, this drawback helped develop a physical intuition for the digital guidance. Nevertheless we find there is a place to consider such a visualization method in a future work.

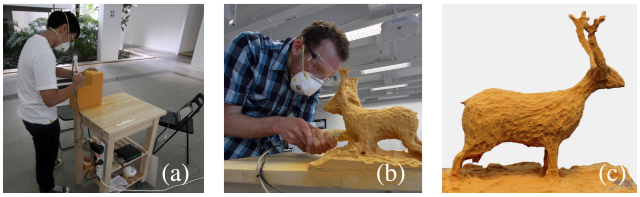

Figure 16. Collaborative effort (a), (b) in creating (c) a deer artifact.

CONCLUSION

We propose a new technique where digital capabilities integrate with handheld carving tools to assist inexperienced makers in carving complex 3D objects, as well as to enable interpretation and modification of a virtual model while fabricating it. The FreeD keeps the user's subjective toolpath as a signature embedded in the texture. In addition, it is capable of completing tasks in a semi-automatic mode, generating a physical texture independently of the user. Since design manipulation is integrated within a tangible carving experience, the nature of this work resembles the process of traditional craft, while allowing risk management and quality assurance.

We wish FreeD to enable creative work in a domain yet unexplored, a new hybrid territory of artifacts produced by both machine and man, fusing automated production with human subjectivity. Blending design with fabrication and automatic process with manual control, we believe the collaborative technology presented here has the potential to alter some of the dominant paradigms in contemporary digital fabrication processes. By introducing traditional approaches to the digital making of artifacts, we hope this intimate collaboration between man and machine will pave the path for a new paradigm in human-computer interaction.

Acknowledgements
Many thanks to our collegues and friends who supported us during the work: T. Rucham, J. Steimle, A. von Kapri, D. Mellis, NW Gong, P. Schmitt, C. Xia, K. Ran, M. Feldmeier, A. Petron, B. Mayton, M. Levin, S. Follmer, Y. Sterman, G. Dublon, N. Gershenfeld, F. Durand, Y. Gingold, L. Liu, M. Gharbi, K. Bala, R. Jaroensri, H.V. Shin, S. Nanayakkara, K.P. Yeo, D. Cohen-Or, and all the craftspersons who shared their knowledge. The CAD models were purchased from turbosquid.com, and the renderings were made with VRay.

REFERENCES

1. Openni user guide. `http://www.openni.org/documentation`, November 2010. Last Checked December 14, 2012.
2. Agarwal, S., and Mierle, K. Ceres solver: Tutorial & reference. `http://code.google.com/p/ceres-solver`, 2012. Last Checked December 14, 2012.
3. Arisandi, R., Takami, Y., Otsuki, M., Kimura, A., Shibata, F., and Tamura, H. Enjoying virtual handcrafting with tooldevice. In *Adjunct proceedings of the 25th annual ACM symposium on User interface software and technology*, ACM (2012), 17–18.
4. Baran, I., and Popović, J. Automatic rigging and animation of 3d characters. In *ACM Transactions on Graphics (TOG)*, vol. 26, ACM (2007), 72.
5. Cho, S., Heo, Y., and Bang, H. Turn: a virtual pottery by real spinning wheel. In *ACM SIGGRAPH 2012 Emerging Technologies*, SIGGRAPH '12, ACM (New York, NY, USA, 2012), 25:1–25:1.
6. Edelsbrunner, H., and Mücke, E. P. Three-dimensional alpha shapes. *ACM Trans. Graph. 13*, 1 (Jan. 1994), 43–72.
7. Follmer, S., Carr, D., Lovell, E., and Ishii, H. Copycad: remixing physical objects with copy and paste from the real world. In *Adjunct proceedings of the 23nd annual ACM symposium on User interface software and technology*, UIST '10, ACM (New York, NY, USA, 2010), 381–382.
8. Gustafson, S., Bierwirth, D., and Baudisch, P. Imaginary interfaces: spatial interaction with empty hands and without visual feedback. In *Proceedings of the 23nd annual ACM symposium on User interface software and technology*, UIST '10, ACM (New York, NY, USA, 2010), 3–12.
9. Hall, M., Frank, E., Holmes, G., Pfahringer, B., Reutemann, P., and Witten, I. H. The weka data mining software: an update. *SIGKDD Explor. Newsl. 11*, 1 (Nov. 2009), 10–18.
10. Johnson, G., Gross, M., Do, E. Y.-L., and Hong, J. Sketch it, make it: sketching precise drawings for laser cutting. In *Proceedings of the 2012 ACM annual conference extended abstracts on Human Factors in Computing Systems Extended Abstracts*, CHI EA '12, ACM (New York, NY, USA, 2012), 1079–1082.
11. McCullough, M. *Abstracting Craft: The Practiced Digital Hand*. MIT Press, Cambridge, MA, USA, 1998.
12. Mueller, S., Lopes, P., and Baudisch, P. Interactive construction: interactive fabrication of functional mechanical devices. In *Proceedings of the 25th annual ACM symposium on User interface software and technology*, UIST '12, ACM (New York, NY, USA, 2012), 599–606.
13. Patel, N. Gestural printing: Jumping the shark on kinect hacks. `http://bit.ly/dLiheh`, 2011. Last checked 11 December, 2012.
14. Rivers, A., Adams, A., and Durand, F. Sculpting by numbers. *ACM Trans. Graph. 31*, 6 (Nov. 2012), 157:1–157:7.
15. Rivers, A., Moyer, I. E., and Durand, F. Position-correcting tools for 2d digital fabrication. *ACM Trans. Graph. 31*, 4 (July 2012), 88:1–88:7.
16. S., C., and Rehg, J. M. Shapeshift: A projector-guided sculpture system. In *Adjunct proceedings of the 20nd annual ACM symposium on User interface software and technology*, UIST '07, ACM (Newport, Rhode Island, USA, October 2007).
17. Sargeant, T. carve. `http://code.google.com/p/carve/`, 2012. Last Checked December 14, 2012.
18. Song, H., Guimbretière, F., Hu, C., and Lipson, H. Modelcraft: capturing freehand annotations and edits on physical 3d models. In *Proceedings of the 19th annual ACM symposium on User interface software and technology*, UIST '06, ACM (New York, NY, USA, 2006), 13–22.
19. Sorkine, O., Cohen-Or, D., Lipman, Y., Alexa, M., Rössl, C., and Seidel, H. Laplacian surface editing. In *Proceedings of the 2004 Eurographics/ACM SIGGRAPH symposium on Geometry processing*, ACM (2004), 175–184.
20. Willis, K. D., Xu, C., Wu, K.-J., Levin, G., and Gross, M. D. Interactive fabrication: new interfaces for digital fabrication. In *Proceedings of the fifth international conference on Tangible, embedded, and embodied interaction*, TEI '11, ACM (New York, NY, USA, 2011), 69–72.
21. Zoran, A., and Paradiso, J. A. Freed – a freehand digital sculpting tool. In *Proceedings of the 2013 ACM annual conference on Human Factors in Computing Systems*, CHI EA '13 (Paris, 2013).